



iJRASET

International Journal For Research in
Applied Science and Engineering Technology



INTERNATIONAL JOURNAL FOR RESEARCH

IN APPLIED SCIENCE & ENGINEERING TECHNOLOGY

Volume: 11 **Issue:** XI **Month of publication:** November 2023

DOI: <https://doi.org/10.22214/ijraset.2023.56909>

www.ijraset.com

Call: ☎ 08813907089

E-mail ID: ijraset@gmail.com

Simulation of Fiber Bragg Grating (FBG) as A Strain Sensor

Muhammad Arif Bin Jalil

Physics Department, Faculty of Science, Universiti Teknologi Malaysia, 81310 Johor Bahru, Johor, Malaysia.

Abstract: In this study, the Fibre Bragg grating (FBG) is modelled, simulated, and characterised with respect to maximum reflectivity, bandwidth, the impact of applied strain on the wavelength shift, λ_B , and the wavelength shift sensitivity with strain for an optical sensing system. This study measures the spectral response of FBG to strain using a commercial FBG with a centre wavelength of 1550 nm. The parameters employed in these simulations include the effective refractive index (1.46), the grating period (Λ) for 530 nm in the FBG performance, the variations in refractive index (Δn) from 0.0002 to 0.0020, and the fibre grating length (L) from 1 to 10 mm. The analysis of the refractive index and grating length variation yields the bandwidth and spectrum reflectivity. OriginPro Software and Microsoft Excel are used to perform simulations on the FBG. Data are generated using the Excel sheet, and visualisations are produced using OriginPro Software. The obtained results show that the bandwidth and spectral reflectivity are impacted by variations in the refractive index and grating length. Furthermore, the obtained results indicate that variations in the Bragg wavelength can be attributed to an elongation of the grating zone caused by the applied strain.

Keywords: Fiber Bragg Grating; Optical Sensor; OriginPro Software; Strain; Maximum Reflectivity; Bandwidth

I. INTRODUCTION

Fibre Bragg Grating (FBG) have shown a great potential advantage in biomedical application over the past ten years [1] due to their prominent characteristics, which include their extremely small size, light weight, immunity to electromagnetic interference (EMI), electrical neutrality, and ability to be easily embedded into a structure without having any effects on the mechanical properties of the object under investigation[2][3]. Fibre Bragg Grating was used as a photoacoustic (PA) detection method to detect the existence of tumours because of its capacity to transform the absorbed energy entirely into heat without producing PA signals caused by scattering particles[4]. Because it combines light contrast and ultrasonic resolution, the photoacoustic approach is unique[5]. This technique is used in tumour diagnosis because of its benefits, which include noninvasiveness, high detection sensitivity, and the ability to identify small element sizes[6],[7].

A sensor can be made out of specifically constructed optical fibre. In a tiny portion of the fibre, the core refractive index of the optical fibre intended for sensor applications differs from that of the conventional fibre core and cladding [8]. Usually, a periodic structure is introduced in that tiny portion of the optical fibre core. Fibre Bragg Gratings (FBG) are the name given to this region of the fibre core because it reflects specific wavelengths of light. When a dielectric waveguide's properties are regularly altered, the effective refractive index of the guide is also periodically altered [9],[10]. Alternatively, when a DBR is a structure composed of multiple, alternating layers of materials with variable refractive indices. The Bragg wavelength shift of Fibre Bragg Gratings determines the sensitivity of FBG-based sensors. Encoded in the fibre core segment, the FBG is a periodic wavelength scale alteration of the refractive index. Bragg gratings reflect light at a particular wavelength that meets the Bragg condition. This reflection in a grating occurs when forward and back propagation modes couple at a specific wavelength [11]. The coupling coefficient of the modes is highest when the specific condition, such as the Bragg condition, between the vectors of the light waves and the vector number of the grating, is satisfied:

$$m \cdot \lambda_B = 2 \cdot n_{eff} \cdot \Lambda \quad (1)$$

For a single FBG, there are theoretically an infinite number of Bragg wavelengths. The diffraction order Bragg wavelength changes for different values of m , as may be obtained from equation (1). In actuality, only one or occasionally two Bragg resonance wavelengths are used because there is a large spectral gap between the two. The second Bragg wavelength of the grating will be twice as short, at 750 nm, assuming the first one, $m=1550$ nm, is 1550 nm. However, the spectral range of the sources utilised for fibre is usually limited to 100 nm.

Additional Bragg peaks may show up if the refractive index modulation in FBG is not sinusoidal, as it usually is. For example, a rectangular grating's Fourier spectrum contains a large number of modulation frequencies, which can result in several Bragg peaks. Even though the index modulation of most fiber-based gratings is essentially sinusoidal. There are several FBG structures; however, in order to test how effectively an FBG works as a sensor, this study's experiment and analysis employed a uniform FBG.

A. The Fundamentals of FBG Sensing Principle.

The Fibre Bragg Grating (FBG) is a single mode fibre having periodic refractive index modulation along its core, as seen in figure 1. When a single mode optical fibre is subjected to intense UV radiation, the reflective index of the fibre core rises, creating a fixed index modulation known as a grating[9]. Since the period of the grating area is approximately half that of the wavelength of the input light, as shown in equation (2) [1][3][8], the wavelength that is reflected when the FBG is subjected to a particular wavelength is known as the Bragg's wavelength, or maximum reflectivity.

$$\lambda_B = 2n_{eff}\Lambda \quad (2)$$

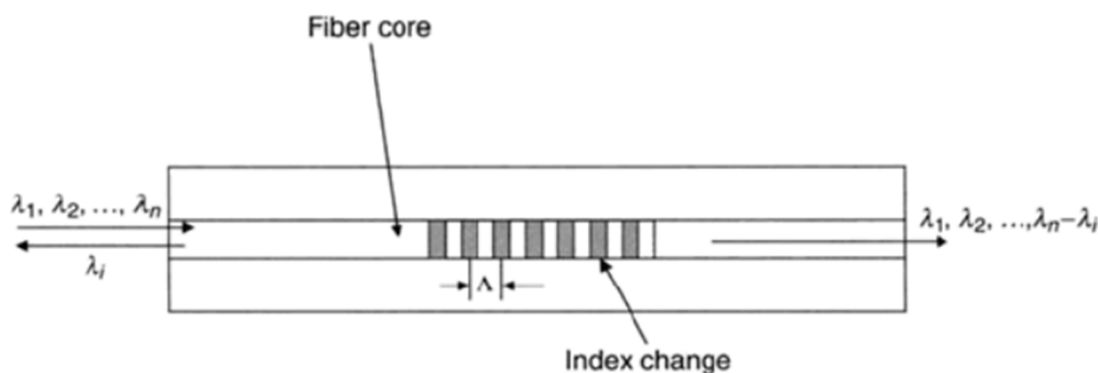


Figure 1: Schematic diagram of a fiber Bragg grating. [14]

Temperature and strain are the two variables in (1) that are sensitive to variations in the outside environment. These parameters are the grating period Λ , the effective index of the core, and the n_{eff} . The effective index is affected by temperature variations due to the thermo-optic effect, whereas the period is affected by thermal expansion of the glass. Hooke's law explains how the elasto-optic effect and the glass elasticity cause changes in period and effective index, respectively, when strain is applied. The effective index and period of the grating will move due to strain and temperature variations, changing the overall Bragg wavelength, λ_B . Therefore, equation (3) will be produced by the Bragg condition:

$$\begin{aligned} \lambda_B + \Delta\lambda_B &= 2 \cdot (n_{eff} + \Delta n_{eff}) \cdot (\Lambda + \Delta\Lambda) \\ &= 2(n_{eff} \cdot \Lambda + n_{eff} \cdot \Delta\Lambda + \Lambda \cdot \Delta n_{eff} + \Delta n_{eff} \cdot \Delta\Lambda) \end{aligned} \quad (3)$$

The last component of the formula can be disregarded since it simply multiplies two little values. After taking (1) into account, we will have the formula for the change in Bragg wavelength:

$$\Delta\lambda_B = 2(n_{eff} \cdot \Delta\Lambda + \Lambda \cdot \Delta n_{eff}) \quad (4)$$

If any of the previously mentioned parameters changes, the Bragg wavelength will also change. By contrasting the related Bragg wavelength shift with the reference, one may identify the alteration.

B. Reflection and Transmission of Light in Fiber Bragg Grating.

As observed in the above image, the refractive index of the fibre core varies with a period of Λ . The part of light whose wavelength coincides with the fiber's wavelength When a broad spectrum light source is discharged into one end of the fibre, the remaining light will pass through to the other end, and the bragg grating will be reflected back to the input end. This reflection phenomena is explained in the diagram below.

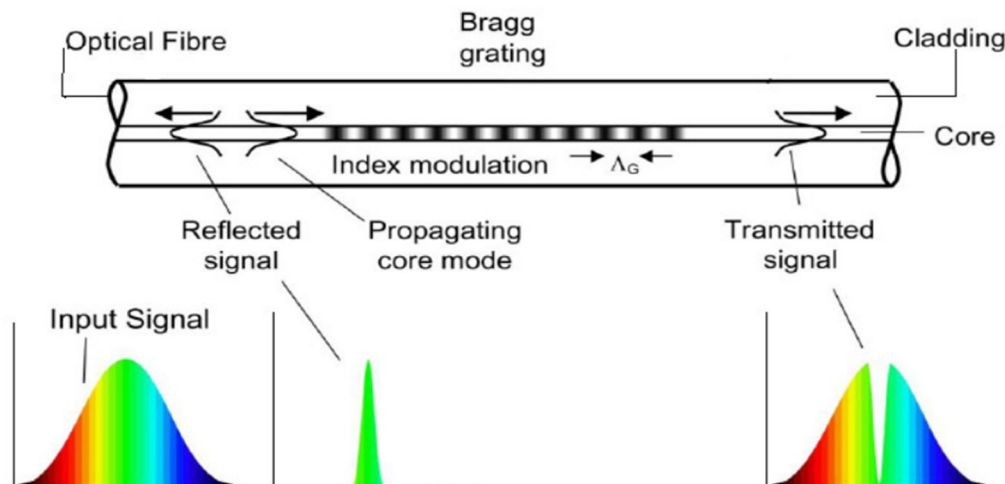


Figure 2 : The reflection and Transmission Spectrum of an FBG. [15]

The necessity of momentum conservation in the Bragg grating condition leads to the following equation:

$$2\left(\frac{2\pi n_{\text{eff}}}{\lambda_B}\right) = \frac{2\pi}{\Lambda} \quad (5)$$

where λ_B is the wavelength of the light reflected by the Bragg grating and n_{eff} is the effective refractive index of the fibre core.

The basic principle behind the functioning of fibre Bragg gratings (FBGs) is Fresnel reflection. When two mediums with different refractive indices come together to allow light to reflect and refract. The fibre Bragg grating will typically show a sinusoidal variation in refractive index over a specified length. As seen in Figure 3, $\Delta\lambda$, where δn_0 is the fluctuation in the refractive index and η is the fraction of power in the core, determines the bandwidth, or the distance in wavelengths between the first minima.

$$\Delta\lambda = \left[\frac{2\delta n_0 \eta}{\pi} \right] \lambda_B \quad (6)$$

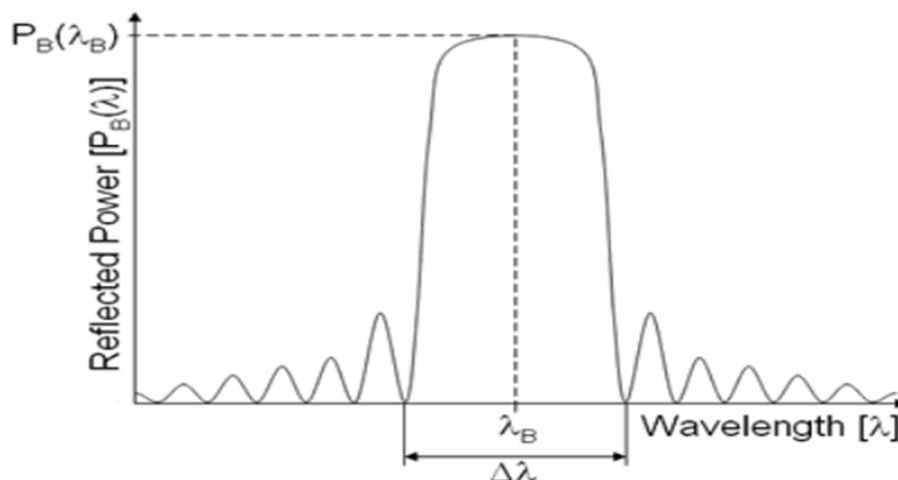


Figure 3: The graph of Reflected Power versus wavelength of a Fiber Bragg Grating. [14]

C. Working Principle of Fiber Bragg Grating.

An optical sensor known as an FBG is produced by laterally exposing a single mode fibre core to a strong UV laser light pattern on a regular basis. The exposure causes the refractive index of the fiber's core to grow gradually, resulting in fixed index modulation that is referred to as grating (Λ) period. As seen in the image below, the grating inside the fibre optic core is responsible for transmitting all other light while reflecting a particular input light wavelength known as the Bragg wavelength (Bragg related to grating period). The Bragg wavelength is given by the equation.

$$\lambda_{Bragg} = 2 \eta \Lambda \quad (7)$$

An interrogating unit, as shown in the above figure, is used to detect the shift in the reflected Bragg wavelength when a change in physical characteristics occurs and is determined by equation.

$$\Delta \lambda_{Bragg} = [(1 - p_e) \cdot \epsilon + (\alpha + \zeta) \cdot \Delta T] \lambda_{Bragg} \quad (8)$$

When p_e is the strain-optic coefficient, T is the change in temperature, induced strain, thermal expansion coefficient, and thermo-optic coefficient are all present. According to the equation above, temperature and strain both affect Bragg shift. $P_e = 0.22$ and various coefficients are known for silica fibre.

D. FBG Equations for Strain Measurement

A sensor's length, or strain, L , varies from its initial length when stress is applied to it. L/L is the equivalent strain over an applied stress to the fibre. Temperature adjustment is required because thermal expansion causes temperature to affect physical dimensions. Strain alone cannot be measured with an FBG sensor unless the impact of temperature on wavelength shift calculations is taken into account. To counterbalance the effect of local temperature on the FBG, this can be achieved by putting a temperature sensor along it. Therefore, we have subtracted eq. (10) from eq. (9) to yield eq. (5) below in order to measure strain.

Equation gives the wavelength shift proportional to the applied strain.

$$\Delta \lambda_{Bragg} = 2 \left(\Lambda \frac{\partial \eta_{eff}}{\partial L} + \eta_{eff} \frac{\partial \Lambda}{\partial L} \right) \times \Delta L \quad (14)$$

$$\Delta \lambda_{Bragg} = \lambda_{Bragg} (1 - p_e) \times \epsilon_z \quad (15)$$

where p is the effective strain-optic constant, denoted as where e is the applied axial strain.

$$p_e = \frac{\eta_{eff}^2}{2} [p_{12} - \nu(p_{11} + p_{12})] \quad (16)$$

where ν is the Poisson's ratio and p_1 and p_2 are parts of the strain-optic sensor. $P_1 = 0.113$, $P_2 = 0.252$, $V = 0.16$, and $N = 1.482$ for a germanosilicate optical fibre. As a result, p has the value 0.22.

Bragg wavelength sensitivity to strain,

$$\frac{\Delta \lambda}{\Delta \epsilon}$$

II. RESULTS AND DISCUSSIONS

In this study, OriginPro software is used to simulate a uniform FBG sensor model in order to acquire the spectrum response. The parameters utilised in the spectral response simulation are listed in Table 1.

Parameters	Symbols	Values
Effective index of refraction	n_{eff}	1.46
Changes in Grating length	L	1 - 10 mm
Bragg's wavelength	λ_B	1550 nm
Variation in index of refraction	Δn	0.0002 - 0.0010
Period of Grating	Λ	530 nm

Table 1: List of main Parameters involved in the simulation of FBG

Strain ($\mu\epsilon$)	Bragg Wavelength, $\lambda_B(\pm 0.10nm)$	Bragg Wavelength shift, $\Delta\lambda_B(\pm 0.01nm)$
0.00	1549.40	0.00
1666.67	1549.60	2.04
3333.33	1549.80	4.08
5000.00	1550.00	6.12
6666.67	1550.20	8.16
8333.33	1550.40	10.21
10000.00	1550.60	12.25
11666.67	1550.80	14.29
13333.33	1551.00	16.34
15000.00	1551.20	18.38
16666.67	1551.40	20.43
18333.33	1551.60	22.47

Table 2: The Bragg wavelength shift with applied strain

A graph of the shift in the Bragg's wavelength against the applied strain is drawn using the estimated values in Table 2 and is displayed in Figure 2 below.

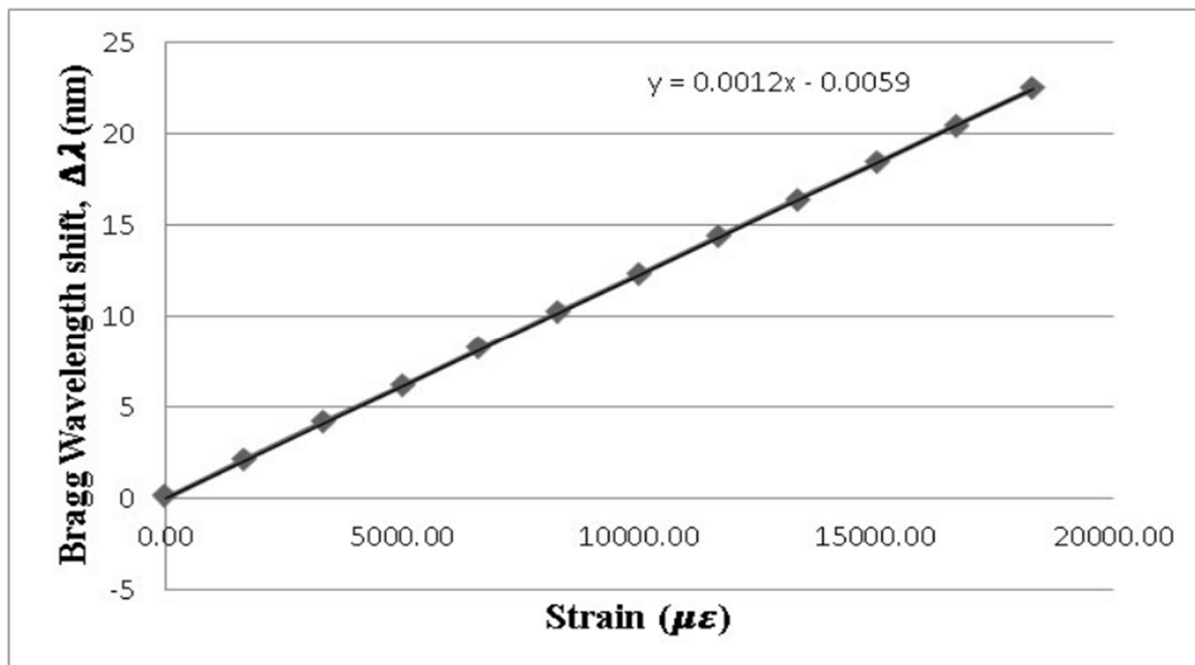


Figure 2: The graph of Bragg wavelength shift against the applied strain

Grating Length (L), mm	$\Delta n = 0.0002$	$\Delta n = 0.0004$	$\Delta n = 0.0006$	$\Delta n = 0.0008$	$\Delta n = 0.0010$
	Reflectivity (R), %				
1.0	15.09	44.84	70.50	85.49	93.33
2.0	44.84	85.49	96.95	99.39	99.89
3.0	70.50	96.95	99.73	99.98	100.00
4.0	85.49	99.39	99.98	100.00	100.00
5.0	93.33	99.89	100.00	100.00	100.00
6.0	96.95	99.98	100.00	100.00	100.00
7.0	98.64	100.00	100.00	100.00	100.00
8.0	99.39	100.00	100.00	100.00	100.00
9.0	99.73	100.00	100.00	100.00	100.00
10.0	99.89	100.00	100.00	100.00	100.00

Table 3: Variation of reflectivity (R) with the variation of grating length (L) and changes in index of refraction (n)

Figure 3 shows that when grating length grows, reflectance increases as well. The FBG obtained 100% reflection when the grating length, L, reached 7 mm and the variations in the index of refraction grew to 0.0004. Additionally, as Table 3 shows, this value holds true for longer grating lengths and larger fluctuations in the index of refraction.

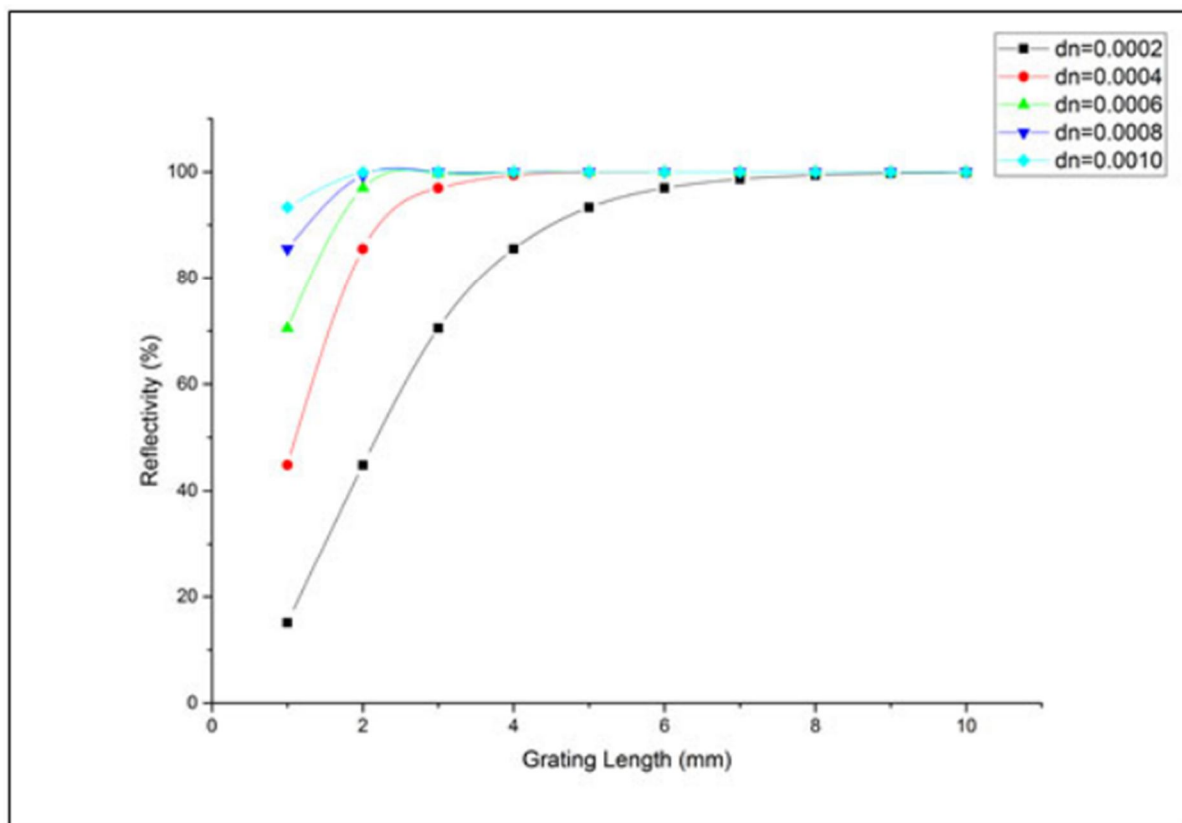


Figure 3: The impact in the variation of grating length (L) and refractive index , ranging from 0.0002 to 0.0010 on reflectivity, (R).

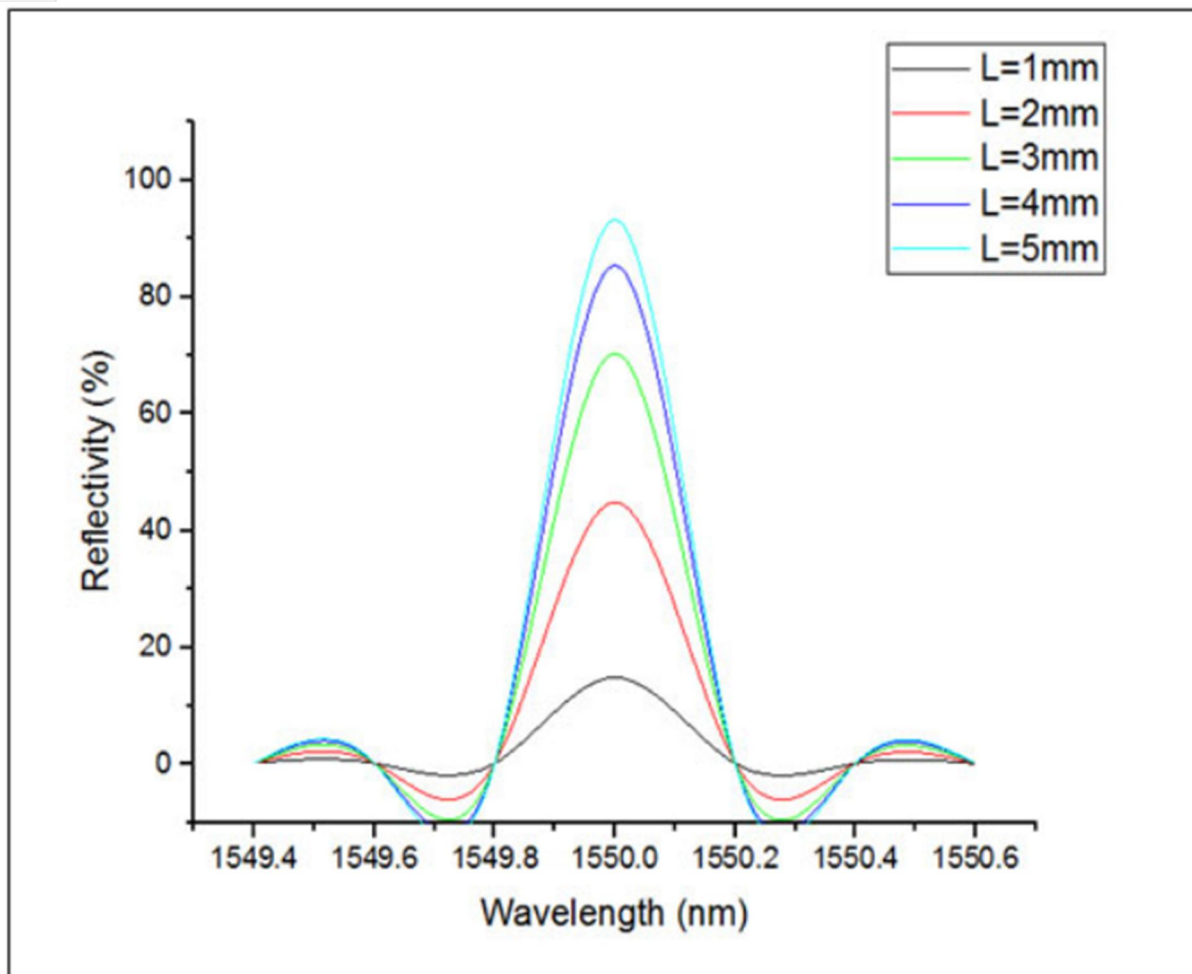


Figure 4: The reflectivity spectrum of a uniform FBG with different value of grating length at constant change in refractive index of $\Delta n = 0.0002$.

A graph of reflectance against wavelength for different grating lengths is shown in Figure 4. The graph clearly shows that grating length increases result in increased reflectivity, which is highly desirable for reflection of FBGs.

III. CONCLUSIONS

In conclusion, the refractive index variation and grating length modifications were used to get the bandwidth and reflectivity spectrum. Additionally, the FBG's effectiveness as a strain sensor was ascertained. According to the simulation results, reflectance rises with increasing grating length and refractive index. When the grating length is increased, the bandwidth of FBG drops, and when the refractive index change is increased, it increases. With OriginPro software, the apodization of the Gaussian profile technique can be used to suppress the sidelobes of spectral reflectivity.

REFERENCES

- [1] E. Al-Fakih, N. A. Abu Osman, and F. R. Mahamd Adikan, "The Use of Fiber Bragg Grating Sensors in Biomechanics and Rehabilitation Applications: The State-of-the-Art and Ongoing Research Topics," *Sensors*, vol. 12, no. 12, pp. 12890–12926, 2012.
- [2] T. Fink, Q. Zhang, W. Ahrens, and M. Han, "Study of π -phase-shifted, fiber Bragg gratings for ultrasonic detection," *Fiber Opt. Sensors Appl.* IX, vol. 8370, no. 7, pp. 1–7, 2012.
- [3] G. Wild and S. Hinckley, "Optical Fibre Bragg Gratings for Acoustic Sensors," *Int. Congr. Acoust.*, no. August, pp. 1–7, 2010.
- [4] A. Yarei and T. Nakanishi, "Fiber Bragg grating applied pulsed photoacoustic detection technique for online monitoring concentration of liquid," *J. Acoust. Soc. Am.*, vol. 123, no. 5, p. 3285, 2008.
- [5] C. Li and L. V Wang, "Photoacoustic tomography and sensing in biomedicine," *Phys. Med. Biol.*, vol. 54, no. 19, pp. R59–R97, 2009.
- [6] M. Xu and L. V. Wang, "Photoacoustic imaging in biomedicine," *Rev. Sci. Instrum.*, vol. 77, no. 4, p. 041101, 2006.
- [7] J. Xia, J. Yao, and L. V Wang, "Photoacoustic Tomography : Principles and Advances," *Prog. electromagnetic Res.*, vol. 147, no. May, pp. 1–22, 2014.



- [8] E.Udd, Fiber Optic Sensors: An Introduction for Engineerings and Scientists (John Wiley and Sons, New York, 1991).
- [9] A.Cusano, A. Cutolo and M. Giordano, "Fiber Bragg Gratings Evanescent Wave Sensors: A View Back and RecentAdvancements", Sensors, Springer-Verlag Berlin Heidelberg, 2008.
- [10] K.O.Hill and G. Meltz, "Fiber Bragg Grating Technology Fundamentals and Overview", Journal of Lightwave Technology, Vol. 15,No. 8, August 1997
- [11] G.P. Agrawal, Fiber-Optic Communication Systems, (John Wiley & Sons, 2002).
- [12] P. Fomitchov and S. Krishnaswamy, "Response of a fiber Bragg grating ultrasonic sensor," Opt. Eng., vol. 42, no. 4, pp. 956–963, 2003.
- [13] M. A. Othman, M. M. Ismail, H. A. Sulaiman, et.al., "An Analysis of 10 Gbits / s Optical Transmission System using Fiber Bragg Grating (FBG)," IOSR J. Eng., vol. 2, no. 7, pp. 55–61, 2012.
- [14] <https://www.fiberoptics4sale.com/blogs/archive-posts/95046406-what-is-fiber-bragg-grating>
- [15] <https://tempsens.com/blog/fiber-bragg-grating-based-sensors>



10.22214/IJRASET



45.98



IMPACT FACTOR:
7.129



IMPACT FACTOR:
7.429



INTERNATIONAL JOURNAL FOR RESEARCH

IN APPLIED SCIENCE & ENGINEERING TECHNOLOGY

Call : 08813907089  (24*7 Support on Whatsapp)